Effective-Interaction Theory of Nuclear Spectral Relations. I. Particle-Hole Relations†

BRUCE J. WEST AND DANIEL S. KOLTUN

Department of Physics and Astronomy, University of Rochester, Rochester, New York 14627

(Received 19 May 1969)

A theory of the relation between particle-particle (pp) and particle-hole (ph) spectra is developed using the effective interaction of the Brueckner-Goldstone many-body theory. The shell-model relation of Pandya, Goldstein, and Talmi is shown to be an approximation to a more general many-particle relation. The main terms omitted by the shell-model pp-ph transformation are found to be of an effective three-body nature. The new theory is applied to the case of ^{42}Sc(pp) and ^{48}Sc(ph), and gives considerably better agreement with experiment than does the standard shell-model relation. For example, the root-mean-square deviation between the predicted and experimental levels of ^{48}Sc is 310 keV for the new theory, as compared to 580 keV for the shell-model relation.

1. INTRODUCTION

RELATIONSHIPS between energy spectra of different nuclei have been obtained in the context of the shell model based on the assumptions that (a) the internucleon potential is strictly a two-body interaction and (b) nuclear states are given by the jj coupling shell model (see, for example, Ref. 1). One well-known relationship of this type is that between a particle-particle (pp) and a particle-hole (ph) spectrum. This relationship will be the subject of this paper.

The pp nucleus refers to two particles in the orbit (jk) outside the closed shell A. The ph nucleus is obtained from the previous nucleus by adding $2k-1$ particles to the orbit k, yielding a nucleus with a particle in the orbit j and a hole k^{-1} in the orbit k "outside" the new core A' which has $A+(2k+1)$ particles.

The energy levels for both the pp nucleus [denoted by $E_J(jk)$] and the ph nucleus $[E_J(jk^{-1})]$ carry the total angular momentum $\mathbf{J}=\mathbf{j}+\mathbf{k}$. We remove from these energies the binding of the two particles (or ph) to the core A (or A') as well as the core energy as follows:

$$E_J=E_{\text{g.s.}}-E_r,$$

where

$$E_r(jk)=-[E_B(A+jk)+E_B(A)-E_B(A+j)-E_B(A+k)], \quad (1.1a)$$

$$E_r(jk^{-1})=-[E_B(A'+jk^{-1})+E_B(A')-E_B(A'+j)-E_B(A'+k^{-1})]. \quad (1.1b)$$

The E_J so defined are often called the interaction energies. The shell model gives the relationship[2]

$$E_J(jk^{-1})=-\sum_I [I]W(jkkj;JI)E_I(jk), \qquad [I]=2I+1. \quad (1.2)$$

This equation is a linear relation between the two spectra which can be inverted to give the pp spectrum in terms of the ph.

We may compare the experimental spectra of two nuclei, which are considered as pp and ph partners through relation (1.2), as a test of the assumptions about the interactions and the purity of the configurations.

The results are shown in Table I for the well-known case of ^{38}Cl and ^{40}K which has a rms deviation of 80 keV between the transformed experimental spectrum of ^{38}Cl using (1.2) and the experimental spectrum of ^{40}K. In the ^{40}K case, the addition of two $0d_{3/2}$ protons to ^{38}Cl forms a ph nucleus with respect to a ^{40}Ca core. The ph reference energy $E_r(jk^{-1})$ is therefore calculated with respect to this core, while the pp reference energy $E_r(jk)$ of ^{38}Cl is calculated with respect to a ^{36}S core. How this change in the core affects the transformed spectrum when a greater number of particles (>2) is needed to go from jk to jk^{-1} is seen by examining the recently acquired spectra of ^{42}Sc [3] and ^{48}Sc [4] which have a ^{40}Ca and ^{48}Ca core, respectively.

Table II shows that the agreement with relation (1.2) is somewhat worse in this latter case; the level spacing is not well predicted, although the J ordering is almost correct. The rms deviation between the predicted and experimental spectrum is now 580 keV. We exhibit this breakdown of (1.2) in a useful form, in terms of the

* Work supported in part by the U. S. Atomic Energy Commission.

[1] I. Talmi and I. Unna, Ann. Rev. Nucl. Sci. **10**, 353 (1960).

[2] S. P. Pandya, Phys. Rev. **103**, 956 (1956); S. Goldstein and I. Talmi, *ibid.* **102**, 589 (1956).

[3] J. J. Schwartz, D. Cline, H. E. Gove, R. Sherr, T. S. Bhatis, and R. H. Siemessen, Phys. Rev. Letters **19**, 1482 (1967).

[4] M. Moinester, J. P. Schiffer, and W. P. Alford, Phys. Rev. **179**, 985 (1969); and (private communication).

TABLE I. The pp-ph transform T of the spectrum of ^{38}Cl compared with the spectrum of ^{40}K (all energies in MeV).

J	$E_J(^{38}\mathrm{Cl})$	$T\{E_J(^{38}\mathrm{Cl})\}$	$E_J(^{40}\mathrm{K})$	ΔE_J
2	−1.687	1.300	1.363	0.063
3	−0.926	0.536	0.593	0.057
4	−0.376	0.472	0.563	0.091
5	−1.012	1.360	1.453	0.093

multipole decomposition of the spectrum,[5] which is discussed in Appendix A. This decomposition takes the form [inverting (A3)]

$$E_J(jk)\equiv\sum_\lambda(-1)^{j+k-J}[jk\lambda]^{1/2}W(jkjk;J\lambda)\alpha^\lambda(jk), \tag{1.3a}$$

where

$$[\lambda]\equiv 2\lambda+1,$$

and $\alpha^\lambda(jk)$ is the strength of the λth multipole. The ph spectrum can be similarly decomposed (as is done in Appendix A) to complete the comparison:

$$E_J(jk^{-1})=\sum_\lambda(-1)^{j+k-J}[jk\lambda]^{1/2}\times W(jkjk;J\lambda)(-1)^{\lambda+1}\alpha^\lambda(jk). \tag{1.3b}$$

Equations (1.3) give a symmetrical representation of the pp-ph relationship (1.2) and its inverse. The Racah transform in (1.2) becomes the phase $(-1)^{\lambda+1}$ in the multipole representation.

Table III gives the multipole strengths for ^{38}Cl and ^{40}K, from which we can see that the largest discrepancy occurs in the $\lambda=0$ or monopole term. The $\lambda=0$ row of Table IV shows the shift in the monopole term for the ^{42}Sc and ^{48}Sc case and is seen to be much greater than the preceding discrepancy of ^{38}Cl and ^{40}K. The relative size of these monopole discrepancies is almost a factor of 7 between the two cases. It is worth noting that the relative increase in the number of three-body interactions involving the odd particle j between the two cases is also seven. It had been noticed some time ago, by Pandya and French,[6] that three-body interactions would violate (1.2). They also showed that configuration mixing, which they calculated for the ^{38}Cl-^{40}K case in perturbation theory, also leads to violations of the relation (1.2).

TABLE II. The pp-ph transform T of the spectrum of ^{42}Sc compared to the spectrum of ^{48}Sc (all energies in MeV).

J	$E_J(^{42}\mathrm{Sc})$	$T\{E_J(^{42}\mathrm{Sc})\}$	$E_J(^{48}\mathrm{Sc})$	ΔE_J
0	−3.200	7.745	6.877	−0.868
1	−2.585	3.193	2.716	−0.477
2	−1.607	1.179	1.347	0.168
3	−1.702	1.245	0.822	−0.423
4	−0.400	0.960	0.453	−0.507
5	−1.682	0.927	0.339	−0.588
6	0.000	0.926	0.197	−0.629
7	−2.575	2.009	1.294	−0.715

[5] See, e.g., J. B. French, in *Proceedings of the International School of Physics "Enrico Fermi," Course 36*, edited by C. Bloch (Academic Press Inc., New York, 1967).

TABLE III. The multipole form of the spectrum of ^{40}K compared to the multipole form of the pp-ph transformed spectrum T of ^{38}Cl (all energies in MeV).

λ	$\alpha^\lambda(^{38}\mathrm{Cl})$	$T\{\alpha^\lambda(^{38}\mathrm{Cl})\}$	$\alpha^\lambda(^{40}\mathrm{K})$	$\Delta\alpha^\lambda$
0	−0.9198	0.9198	1.0005	0.0807
1	0.1546	0.1546	0.1663	0.0117
2	−0.3905	0.3905	0.3888	−0.0017
3	−0.0408	−0.0408	−0.0477	−0.0069

In this paper, we develop a general theory of the relation of pp and ph spectra, based on the effective interaction developed in the Brueckner-Goldstone many-body theory of nuclei. The present theory isolates the cause of the violation of relation (1.2), and provides a direct method of calculating this violation. In the theory of the effective interaction, configuration mixing is formally removed from the nuclear wave function, and is included in the structure of the effective interaction itself. In this language, the violation of relation (1.2) can be traced to the fact that the effective interaction between valence particles is no longer a two-body interaction. We find the leading contributions to the many-particle interaction which causes the violation of relation (1.2) are of two types: (i) those which depend on *which* closed-shell nucleus is treated as the core and (ii) those that have an effective three-body character. This latter case is due to configuration admixtures unique to one end of the valence shell.

We introduce the pp-ph transformation of a set of numbers $M(jk;J)$ (e.g., energies), for all J ($|j-k|\leq$

TABLE IV. The multipole form of the spectrum of ^{48}Sc compared to the multipole form of the pp-ph transformed spectrum T of ^{42}Sc (all energies in MeV).

λ	$\alpha^\lambda(^{42}\mathrm{Sc})$	$T\{\alpha^\lambda(^{42}\mathrm{Sc})\}$	$\alpha^\lambda(^{48}\mathrm{Sc})$	$\Delta\alpha^\lambda$
0	−1.432	1.432	0.895	−0.537
1	−0.095	−0.095	−0.250	−0.155
2	−0.731	0.731	0.761	0.030
3	−0.246	−0.246	−0.223	0.023
4	−0.446	0.446	0.362	−0.084
5	−0.322	−0.322	−0.222	0.100
6	−0.296	0.296	0.223	−0.073
7	−0.101	−0.101	−0.163	−0.062

[6] S. P. Pandya and J. B. French, Ann. Phys. 2, 166 (1957).

$J \leq j+k$):

$$T\{M(jk;J)\} = -\sum_{J'} [J'] W(jkkj;JJ') M(jk;J'). \tag{1.4}$$

An operator which *conserves* the pp-ph transformation is one for which the ph matrix elements is given by (1.4):

$$\langle jk^{-1};J \mid \mathfrak{M}_c \mid jk^{-1};J\rangle = T\{\langle jk;J \mid \mathfrak{M}_c \mid jk;J\rangle\}. \tag{1.5}$$

In Sec. 2 we introduce the valence effective interaction $\mathcal{U}$ and show that it can be divided into a conserving (c) and violating (v) part

$$\mathcal{U} = \mathcal{U}_c + \mathcal{U}_v, \tag{1.6}$$

where $\mathcal{U}_c$ obeys (1.5).

We can now define the experimental spectral violation of the pp-ph relationship (1.2) in terms of (1.5):

$$\Delta E_J \equiv E_J(\text{ph}) - T\{E_J(\text{pp})\}. \tag{1.7}$$

In Sec. 3 we discuss the characteristics of the violating terms, which contribute to $\mathcal{U}_v$. We shall show that these terms correspond to many-particle contributions to the valence effective interaction.

In Sec. 2 we define criteria by which individual Brueckner-Goldstone diagrams for $\mathcal{U}$ (or their equivalent terms in a perturbation series) are classified as belonging either to $\mathcal{U}_c$ of $\mathcal{U}_v$. In Appendix B, we prove that the pp diagrams which fall into the class $\mathcal{U}_c$ in fact are related to specific ph diagrams by the relation between their matrix elements given by (1.5).

For pp-ph conjugate nuclei discussed above, the violation of the transformation (1.2) is an order of magnitude smaller than the average splitting of the levels. We therefore expect that $\mathcal{U}_v$ can be treated as a perturbation on $\mathcal{U}_c$. This is done specifically in Sec. 4 and applied to the conjugate nuclei ^{42}Sc and ^{48}Sc. The calculation is done using matrix elements for $\mathcal{U}_c$, which have been calculated and published by other groups. These matrix elements were not available for the ^{38}Cl-^{40}K case. The calculation of $\mathcal{U}_v$ for the Sc case accounts for the experimental discrepancies, as can be seen in Tables V–IX and Figs. 1 and 2.

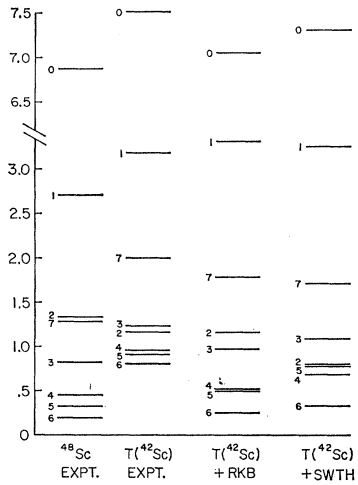

FIG. 1. The columns represent, in order from left to right, the experimental spectrum of ^{48}Sc, the ph-transformed spectrum of ^{42}Sc. and the corrected spectrum using the RKB and SWTH matrix elements, respectively, in the matrix calculation.

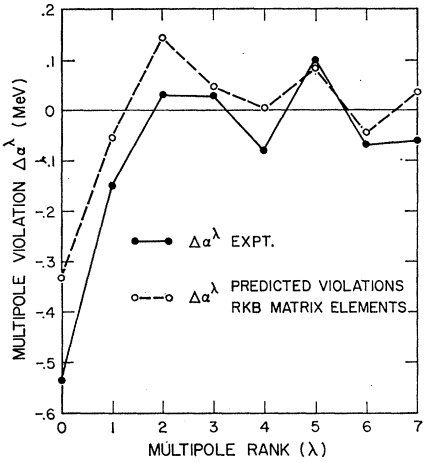

FIG. 2. The violation of the pp-ph relation (1.2) in terms of multipoles $\Delta\alpha^\lambda$: Solid circles are the experimental differences, and open circles the calculated differences, using the RKB matrix elements.

2. TRANSFORMATION PROPERTIES OF $\mathcal{U}$

In this section we investigate the valence effective interaction $\mathcal{U}$ and its separation into $\mathcal{U}_c$ and $\mathcal{U}_v$, according to (1.5) and (1.6). A definition of this shell-model effective interaction, based on a development of the Brueckner-Goldstone many-body perturbation theory, has been given by Bloch and Horowitz.[7] This form of the interaction among valence particles is energy-dependent, and may be written

$$\mathcal{U}(E_v) = \sum_{p=0}^{\infty} V\{[Q/(E_v - H_0)]V\}^p, \tag{2.1}$$

where H_0 is the single-particle Hamiltonian with kinetic energy T, potential energy U, and

$$H_0 = T + U.$$

The total Hamiltonian for the system is written

$$H = T + V_2 = H_0 + V,$$

where V_2 is the free two-nucleon interaction and $V = V_2 - U$.

The energy E_v in the denominator of (2.1) is given by

$$E_v = E_0 + \Delta E_v,$$

[7] C. Bloch and J. Horowitz, Nucl. Phys. **8**, 91 (1958).

where E_0 is the sum of the single-particle energies (given by H_0) and ΔE_v is the interaction energy of the valence particles in an eigenstate of $\mathcal{U}(E_v)$. For example, for the case of two valence particles j and k, in a state of total angular momentum J, the interaction energy is given by the matrix element

$$\Delta E_J(jk) \equiv \langle jk; J \mid \mathcal{U}(E_v) \mid jk; J \rangle. \quad (2.2)$$

This approach is reviewed by Brandow[8] and by MacFarlane.[9]

Brandow[8] has also extended the Bloch-Horowitz formalism to eliminate from the valence effective interaction contributions from "unlinked terms" in (2.1). This *linked-valence* formalism leads to an expression for $\mathcal{U}(E_v)$ similar to (2.1), from which the interaction energies ΔE_v in the denominators are removed:

$$\mathcal{U} = \sum_{p=0}^{\infty} V\{[Q/(E_0 - H_0)]V\}_{\text{l.v.}}{}^p. \quad (2.1')$$

Brandow has shown that the contributions of ΔE_v in (2.1) is canceled by the unlinked terms, so that one may obtain the reduced expansion (2.1′) with only linked-valence terms (denoted by l.v.). The notion of linked and unlinked *terms* comes about through examining the diagrammatic representation of (2.1) and (2.1′) and associating with each perturbation term either a linked or unlinked *diagram* (see Refs. 8 and 10).

For the purposes of this section, the distinction between the expansions shown in (2.1) and (2.1′) is not important. It will be important, however, in treating the specific contributions to the violating interaction (Secs. 3 and 4). In calculating the contributions to $\mathcal{U}_v$, we shall use the linked-valence form of the effective interaction (2.1′).

Now we shall consider a specific set of terms of (2.1) and show that they contribute to the conserving interaction $\mathcal{U}_c$. In the process of construction, we shall demonstrate the essential characteristics which define the terms of $\mathcal{U}_c$.

Consider first the terms corresponding to the "Brueckner ladder diagrams" which for two valence particles, or valence p and h, have intermediate states with two particles excited above the valence shell. We may write the subseries of (2.1) for the two cases

$$\mathcal{U}_B(\text{pp}) = \sum_{q=0}^{\infty} V_2\{[Q(\text{pp})/(E - H_0)]V_2\}^q, \quad (2.3a)$$

$$\mathcal{U}_B(\text{ph}) = \sum_{q=0}^{\infty} V_2\{[Q(\text{2p-2h})/(E' - H_0')]V_2\}^q, \quad (2.3b)$$

where the projection operator $Q(\text{pp})$ allows no valence particles in the intermediate states, and $Q(\text{2p-2h})$ has the same two particles as in $Q(\text{pp})$, in addition to *two* valence holes. The subscripts are omitted from the energies E and E' to emphasize that (2.1) and (2.1′) are treated as equivalent in the following.

The terms of (2.3a) correspond to the usual Brueckner "ladder" diagrams [Fig. 3(a)], which are all linked. Each term of (2.3b), however, contains both a ph ladder diagram [Fig. 3(b)] and a disconnected term [Fig. 3(c)]. This second term is canceled by a shift in the single-particle potential U of H_0, for the filled-valence-shell case relative to the empty-valence-shell case. This absorption of the disconnected diagrams into the single-particle potential is already present in the usual form of the pp-ph transformation, to first order in V_2 [see (A6)]. We note that this effect has been included by allowing the single-particle spectrum given by H_0' in the ph case (2.3b) to differ from that in the pp case (2.3a).

Because of the differences in the Q operators and single-particle spectra in (2.3a) and (2.3b), the operators $\mathcal{U}_B(\text{pp})$ and $\mathcal{U}_B(\text{ph})$ are quite distinct. However, we shall now show that under certain conditions, we can construct a *single* operator $\mathcal{U}_B$ which has the same matrix elements as each of the operators (2.3a) and (2.3b); that is,

$$\langle jk; J \mid \mathcal{U}_B \mid jk; J \rangle = \langle jk; J \mid \mathcal{U}_B(\text{pp}) \mid jk; J \rangle, \quad (2.4a)$$

$$\langle jk^{-1}; J \mid \mathcal{U}_B \mid jk^{-1}; J \rangle = \langle jk^{-1}; J \mid \mathcal{U}_B(\text{ph}) \mid jk^{-1}; J \rangle. \quad (2.4b)$$

The first aim in this construction is to find the conditions under which we can eliminate the Q operators in (2.3), which distinguish the two $\mathcal{U}_B$ operators. We use the second-quantized form of V_2 given in (A1) of Appendix A:

$$V_2 = \sum_{lmnr,J} [J]^{1/2} \langle lm; J \mid V_2 \mid nr; J \rangle \times [(A_l \times A_m)^J \times (B_n \times B_r)^J]^0, \quad (2.5)$$

where the A's and B's are the spherical-tensor single-particle creation and destruction operators, and $(A_l \times A_m)^J$ creates two-particle states l and m coupled to total angular momentum J.

The projection operators Q for a specific term in the series (2.3) tell us which single-particle states are allowed in the intermediate states, e.g., α, $\beta \neq j$, k in Fig. 3. We may alternatively accomplish the same

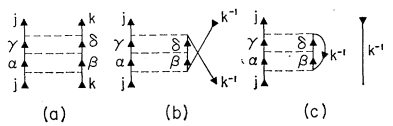

FIG. 3. (a) Third-order "ladder" diagram for $\mathcal{U}_B$ in the pp case. Upon transformation $k \to k^{-1}$, (a) goes to (b)+(c). The disconnected term (c) is absorbed into the single-particle energy of particle j.

[8] B. H. Brandow, Rev. Mod. Phys. **39**, 771 (1967).
[9] M. H. Macfarlane, in *Proceedings of the International School of Physics "Enrico Fermi," Course 40* (Academic Press Inc., New York, to be published).
[10] J. Goldstone, Proc. Phys. Soc. (London) **A239**, 267 (1956).

restriction by selecting only the appropriate terms of the expression (2.5) for the interaction. Then Q becomes redundant, and may be replaced by unity. Explicitly we consider the two subseries of (2.5):

$$W_1=\sum_{\alpha,\beta,J}[J]^{1/2}\langle\alpha\beta;J\mid V_2\mid jk;J\rangle \times\{[(A_\alpha\times A_\beta)^J\times(B_j\times B_k)^J]^0 +[(A_j\times A_k)^J\times(B_\alpha\times B_\beta)^J]^0\}, \quad (2.6a)$$

$$W_2=\sum_{\alpha\beta\gamma\delta,J}[J]^{1/2}\langle\alpha\beta;J\mid V_2\mid\gamma\delta;J\rangle \times[(A_\alpha\times A_\beta)^J\times(B_\gamma\times B_\delta)^J]^0, \quad (2.6b)$$

where none of the indices α, β, γ, or δ can be either j or k.

We now construct an operator $\mathcal{V}_B$ defined by

$$\mathcal{V}_B\equiv V_2+W_1\sum_{q=0}^{\infty}(d^{-1}W_2)^q d^{-1}W_1. \quad (2.7)$$

Clearly, this operator has the same valence matrix elements as in the sense of (2.4a), if we set $d\equiv E-H_0$. But the operator also has the same valence matrix elements as $\mathcal{V}_B$(ph) [see (2.4b)], if we set $d\equiv E'-H_0'$.

We can also use the explicit forms (2.6) to rewrite the qth term in the series (2.7) in the form

$$\mathcal{V}_B{}^{(q)}=\sum_{IJ,r}\{[(A_j\times A_k)^I\times(B_\alpha\times B_\beta)^I]^0M(q) \times[(A_\gamma\times A_\delta)^J\times(B_j\times B_k)^J]^0\}, \quad (2.8)$$

where $M(q)$ is a scalar operator

$$M(q)=[IJ]^{1/2}\langle jk;I\mid V_2\mid\alpha\beta;J\rangle \times(d^{-1}W_2)^{q-1}d^{-1}\langle\gamma\delta;J\mid V_2\mid jk;J\rangle. \quad (2.9)$$

We can recouple (2.8) in the form

$$\mathcal{V}_B{}^{(q)}=\sum_{IJ,r}\{[(A_j\times A_k)^I\times N^r]^J\times(B_j\times B_k)^J\}^0, \quad (2.10)$$

where the tensor operator N^r, of rank r, contains $M(q)$ and the A and B operators of (2.8) for α, β, γ, δ, and the recoupling (Racah) coefficients.

Notice that N^r contains only creation and destruction operators, e.g., A_α, B_β for unoccupied single-particle states. Therefore, in the valence matrix elements (2.4) only the scalar N^0 can, in fact, contribute, since in these matrix elements, we have a "vacuum" for the unfilled shells; therefore

$$\langle 0\mid N^r\mid 0\rangle=\langle 0\mid N^0\mid 0\rangle\delta_{r0}. \quad (2.11)$$

It follows that for valence matrix elements, (2.10) reduces to

$$\mathcal{V}_B{}^{(q)}=\sum_I\langle 0\mid N^0\mid 0\rangle[(A_j\times A_k)^I\times(B_j\times B_k)^I]^0. \quad (2.12)$$

Now $\mathcal{V}_B{}^{(q)}$ acts as a two-body scalar interaction operator in the valence space, of the form (2.5). Following the argument of Appendix A [see (A8)], we find that $\mathcal{V}_B$ obeys the pp-ph theorem (1.5).

Therefore, we can use the pp-ph theorem (1.5) for every term in the Brueckner ladder series (2.3) for which $d=E'-H_0'\approx E-H_0$. This is a good approximation for intermediate states with energies well above the valence shells. What is required is that the change in the energy denominators, from the pp to the ph case, be small compared to the denominators themselves. We expect the relative change to be of the order of a few MeV, so the minimum excitation energy for the approximation to be good would be of the order $\sim$30 MeV ($\sim 2\hbar\omega$ in an oscillator model).

This leads us to separate the intermediate states in (2.3) into *high-lying* and *low-lying* states. The former are defined as those states with (a) two particles excited outside the valence shells and with (b) excitation energy E_0-H_0 larger than some minimum, for example, $2\hbar\omega$. The *low-lying* intermediate states violate either one or both conditions. For the ph case (2.3b), the *high-lying* states have two valence holes, in addition to the excited particles. A term in the perturbation series will be referred to as either high-lying or low-lying depending on the intermediate state in that term.

We conclude that, to a good approximation, the Brueckner effective interaction (ladder diagrams) matrix elements (2.4) obey the pp-ph transform (1.5), *if* we include only the high-lying terms. This elimination of intermediate states close to the valence shell appears in most practical calculations of $\mathcal{V}_B$. For example, Kuo and Brown[11] consider only intermediate states of high excitation, which are treated as plane waves in calculating their "bare" interaction. Becker and MacKellar[12] have similarly suppressed low-lying states through their approximate Pauli principle.

Now let us consider more general terms in the valence effective interaction (2.1). We write

$$\mathcal{V}(\text{pp})=\mathcal{V}_c(\text{pp})+\mathcal{V}_v(\text{pp}), \quad (2.13a)$$

$$\mathcal{V}(\text{ph})=\mathcal{V}_c(\text{ph})+\mathcal{V}_v(\text{ph}), \quad (2.13b)$$

where the terms in $\mathcal{V}_c$(pp) and $\mathcal{V}_c$(ph) are related by (1.5). Again, we shall construct an operator $\mathcal{V}_c$ which has the same matrix elements as $\mathcal{V}_c$(pp) and $\mathcal{V}_c$(ph) as follows:

$$\langle jk;J\mid\mathcal{V}_c\mid jk;J\rangle=\langle jk;J\mid\mathcal{V}_c(\text{pp})\mid jk;J\rangle, \quad (2.14a)$$

$$\langle jk^{-1};I\mid\mathcal{V}_c\mid jk^{-1};I\rangle=\langle jk^{-1};I\mid\mathcal{V}_c(\text{ph})\mid jk^{-1};I\rangle. \quad (2.14b)$$

A sufficient condition that a term in $\mathcal{V}$ contribute to $\mathcal{V}_c$ is that it may be written in the form (2.10), where N^r is a tensor operator of rank r, which may have creation and destruction operators for any number of particles in any state other than the valence states j or k. Of course, N^r must be identical in the pp and ph cases. Under such conditions, we may again follow the

[11] T. T. S. Kuo and G. E. Brown, Nucl. Phys. **85**, 40 (1966).
[12] R. L. Becker and A. D. MacKellar, Phys. Letters **21**, 201 (1966).

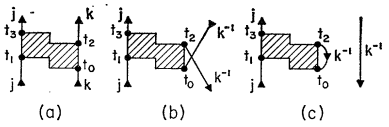

FIG. 4. Diagram (a) is of the general form of a diagram contributing to $\mathcal{U}_c(\mathrm{pp})$. Upon transformation $k\rightarrow k^{-1}$, diagram (b) contributes to the interaction $\mathcal{U}_c$ (ph), while (c) is absorbed into the single-particle energy. Figure 3 is a special example of this figure.

steps leading to (2.12), and therefore to the transformation (1.5) of the matrix element of (2.14).

We shall prove (in Appendix B) that terms in $\mathcal{U}$ which obey the following two conditions can be written in the form (2.10), with constant N^r, and therefore are terms in $\mathcal{U}_c$: (a) The condition that a term in $\mathcal{U}_c$ can be written in the form (2.10) is equivalent to requiring that in that term, each particle in a valence shell (j, k) interacts exactly twice, and between the two interactions no particle is in *that* valence shell (j, k). We work in a *np* formalism so the neutron and proton valence shells are always distinct. For the ph case, between the two interactions of the valence hole (k^{-1}), two (and only two) k-hole states will be present. See Fig. 4 for clarity. (b) The second condition mentioned, that N^r must be identical in the pp and ph cases, can be satisfied to the extent that the energy denominators $E-H_0$ and $E'-H_0'$ are equal. These two conditions are a generalization of the definition of *high-lying* which we applied to intermediate states of the Brueckner ladder terms. Here we shall refer to a *term* in $\mathcal{U}$ which satisfies both properties (a) and (b) as a *high-lying term*. We note that the condition (b) on the equality of energy denominators can, in fact, always be *formally* satisfied, since we are free to adjust H_0 and H_0' in the theory. Such adjustments are compensated by higher-order terms in the violating effective interaction $\mathcal{U}_v$.

In Appendix B we give a proof, in terms of Goldstone diagrams, that these terms, which we have called high-lying, in fact transform as (1.5), and therefore belong to $\mathcal{U}_c$. Some examples are shown in Fig. 5. Diagrams 5(a) and 5(a′) stand for the Brueckner ladder series (2.3a) and (2.3b), respectively (reaction matrix $\mathcal{U}_B$). The rest of the figure shows contributions to $\mathcal{U}_c$ which are of second order in $\mathcal{U}_B$. For each letter, there is a pp diagram (x) and its ph transform (x′). Note that here $\alpha, \beta \neq j, k$. We also assume that the excitation energies of α, β are sufficient, so that all the diagrams are *high-lying*.

The terms in $\mathcal{U}$ which are high-lying contribute to the violating valence interaction $\mathcal{U}_v$, which contributes to the spectral violation (1.7) by

$$\Delta E_J = \langle jk^{-1}; J \mid \mathcal{U}_v(\mathrm{ph}) \mid jk^{-1}; J\rangle - T\{\langle jk; J \mid \mathcal{U}_v(\mathrm{pp}) \mid jk; J\rangle\}. \quad (2.15)$$

In order to calculate the violating terms in $\mathcal{U}_v$, we reorder the original series (2.1) in powers of $\mathcal{U}_c$:

$$\mathcal{U}_v = \mathcal{U} - \mathcal{U}_c = \mathcal{U}_c[\tilde{Q}/(E-H_0)]\mathcal{U}_c + O(\mathcal{U}_c^3), \quad (2.16)$$

where $\tilde{Q}$ now projects only onto *low-lying* excited states. We expect to be able to account for $\mathcal{U}_v$ by the leading terms of the "perturbation" series (2.16), in those cases where the experimental $|\Delta E_J|$ are smaller than the order of magnitude of the level splittings, as in the cases discussed in the Introduction.

In the next section, we discuss the essential characteristics of the leading terms in $\mathcal{U}_v$.

3. GENERAL CHARACTERISTICS OF VIOLATING TERMS

The terms in $\mathcal{U}_v$ are those which do not satisfy *both* conditions in the definition, given in Sec. 2, of *high-lying* terms. There are terms (diagrams) which contribute to $\mathcal{U}_v$ only because of significant changes in energy denominators, between the pp and ph cases. There is a second category of terms (diagrams) which involve intermediate states containing valence particles (or holes), but which can only occur at one end of the valence shell. These latter terms may be thought of as due to a blocking effect; they appear as contributions of an effective three-body valence interaction.

The terms in the first of the two categories have the same diagrammatic structure as the terms in $\mathcal{U}_c$, and they *would* transform if not for the shift in the energy denominators due to the change in cores. To explain this more fully, consider diagram (a) of Fig. 6. Its contribution to the energy in the pp case is

$$E_J^{(v)}(jk) = \frac{|\langle jk; J \mid \mathcal{U}_c \mid \alpha\beta; J\rangle|^2}{E_{\alpha\beta}},$$

$$E_{\alpha\beta} = E_j - E_\alpha + E_k - E_\beta \quad (3.1)$$

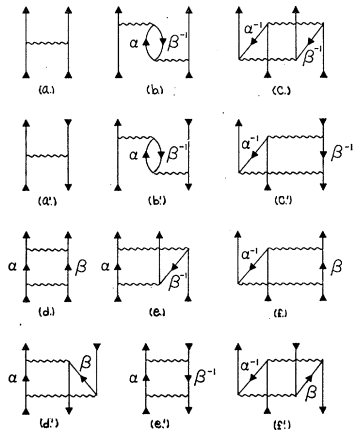

FIG. 5. (a)–(f) Some of the second-order contributors to the series expansion for $\mathcal{U}_c$. The unprimed and primed diagrams are related through the ph transformation, the primed being those that occur in the series expansion in the ph case.

and transforming this to the ph case ($k \to k^{-1}$) gives

$$T\{E_J^{(v)}(jk)\} = T\left\{\frac{|\langle jk; J \mid \mathcal{V}_c \mid \alpha\beta; J\rangle|^2}{E_{\alpha\beta}}\right\}, \quad (3.2)$$

which is a well-defined contribution to the ph energy.

If we now consider the corresponding diagram in the ph case [Fig. 6(b)], a term of similar form to (3.2) arises but with a different energy denominator, reflecting the change in the single-particle energies:

$$E_{J'}^{(v)}(jk^{-1}) = \frac{\langle jk^{-1}; J' \mid \mathcal{V}_c Q_{\alpha\beta} \mathcal{V}_c \mid jk^{-1}; J'\rangle}{E_{\alpha\beta}+\Delta_\alpha+\Delta_\beta}, \quad (3.3)$$

where

$$\Delta_\alpha = (E_j - E_\alpha)_{\rm ph} - (E_j - E_\alpha)_{\rm pp},$$

$$\Delta_\beta = (E_k - E_\beta)_{\rm ph} - (E_k - E_\beta)_{\rm pp}.$$

The contribution to the total correction to the transformed pp spectrum may be put in the form

$$\Delta E_J = E_J^{(v)}(jk^{-1}) - T\{E_J^{(v)}(jk)\}$$

$$= -\frac{\Delta_\alpha+\Delta_\beta}{E_{\alpha\beta}+\Delta_\alpha+\Delta_\beta} T\left\{\frac{|\langle jk; J \mid \mathcal{V}_c \mid \alpha\beta; J\rangle|^2}{E_{\alpha\beta}}\right\}, \quad (3.4)$$

where we have combined (3.2) and (3.3) using (A4) and (A10). We call the coefficient of the transformed terms the dilution factor. This factor indicates the single-particle energy dependence of the contributions due to the low-lying states. It also gives a measure of the validity of the separation into low- and high-lying intermediate states; the factor becomes zero for the high-lying states. For example, Kuo and Brown have found that intermediate states of excitation energy of about 200 MeV above the valence shell give the major contribution to the "dispersion term" in the "bare" Brueckner interaction [see Eq. (2.3)].[11] Since the shifts in the single-particle energies between the pp and ph cores are approximately 2 MeV, one expects no more than a 1% violating effect from the dilution (3.4). For this reason, we neglect violating contributions from the high-lying states and in $\mathcal{V}_c$.

The second type of violating diagram occurs in both the pp and ph case and is a consequence of configuration admixtures that are unique to one end of the shell. Consider the ph diagram (a) of Fig. 7, which is a single-particle excitation. This diagram cannot be obtained by a transformation of a pp diagram. This is due to the fact that in the latter case, the core contains no particles

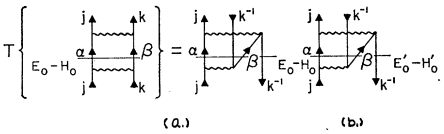

FIG. 6. This diagram transforms according to (1.2), but is *low-lying*. The energy denominator in the propagator for(a) is not the same as that for (b) because of the additional interactions that are possible with the extra $2k-1$ particles in (b).

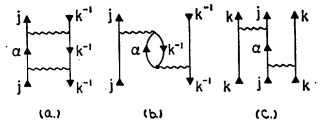

FIG. 7. Three-body character of ph diagrams (a) and (b), in which only one particle is excited outside the valence shells. (c) Three-particle term, contained in (a) and (b), where we replace the k^{-1} line by $2k$ particle lines (filled shell -1).

in the k shell, so that the intermediate state may not have a single k hole. One might also view this as an effect of the Pauli principle, which prevents putting two k particles into the state of one k hole.

It is instructive to consider the hole in this diagram as a filled shell minus one particle. In these terms, the diagram equivalent to Fig. 7(a) will contain the three-particle interaction shown in Fig. 7(c). Thus Fig. 7(a) is seen to include effective three-body terms which would not be expected to appear in a corresponding pp diagram. This same argument applies to Fig. 7(b), so that it also contains effective three-body terms. The fact that a single-particle excited state contributes to an effective three-body interaction appears to have been first recognized by Bacher and Goudsmit.[13] Three-body terms of the form of Fig. 7(c) have also been recognized by Osnes[14] and by Bertsch[15] and their contributions to the binding energy of nuclei in the Ca-Ni region have been calculated.

Similar contributions come from pp diagrams which do not transform into ph diagrams. For example, diagrams (d) and (f) of Fig. 5 exist for which $\beta = k$, but the transformed diagrams (d') and (f') do not exist in this case. Now the "three-body" effect involves two k holes and one j particle, which is also a Pauli-principle effect.

The contribution of $\mathcal{V}_v$ to the spectral violation of the ph relationship (1.2) is calculated as in (2.15). One computes the matrix elements of the violating diagrams for the ph case. From these, one subtracts the transform (1.5) of the matrix elements for the violating diagrams for the pp case.

We remark, in conclusion, that the three-body terms discussed in connection with Fig. 7 are the leading terms in a perturbation expansion of $\mathcal{V}_v$. Higher-order terms will bring in interactions involving even higher numbers of particles. In fact, the *dilution* terms discussed first [Eq. (3.4)] already result from many-body effects, which appear in the changes of the single-particle spectra between the pp and ph nuclei.

4. CALCULATIONS AND RESULTS

We now turn to the calculation of the violating terms in ΔE_J [Eq. (2.15)] for the conjugate pair ^{42}Sc(pp) and ^{48}Sc(ph). We have already exhibited the experi-

[13] R. F. Bacher and S. Goudsmit, Phys. Rev. **46**, 948 (1934).
[14] E. Osnes, Phys. Letters **26B**, 274 (1968).
[15] G. F. Bertsch, Phys. Rev. Letters **21**, 1694 (1968).

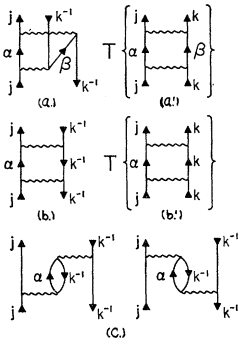

FIG. 8. (a)–(c) occur in ^{48}Sc and violate the ph transformation; (a′) and (b′) occur in ^{42}Sc. The T denotes that their matrix elements have been transformed to ^{48}Sc. Diagrams (a) and (a′) violate due to energy denominators, whereas the remaining diagrams violate because of their effective three-body character.

mental discrepancies [Eq. (1.7)] in Table II. We may compare theoretical results with experiment in several ways:

(a) We may compare the calculated values of ΔE_J with the experimental discrepancies in Table II. This is done in Table VI.

(b) Alternatively, we may compare calculated and experimental multipole differences (see Table IV). This is also done in Table VI (see also Fig. 2).

(c) We may add the calculated values of ΔE_J to the transformed [by (1.2)] spectrum of ^{42}Sc as indicated by (2.15), and compare the resulting values to the experimental spectrum of ^{48}Sc. This is done in Fig. 1. As a measure of the improvement, we compare the rms deviation between the experimental spectrum and our theoretical predictions to the rms deviation between experiment and transformed spectrum of ^{42}Sc using only (1.2). This is done in Table VII.

The model for ^{42}Sc is a neutron and proton in the $0f_{7/2}$ shell outside a ^{40}Ca closed shell. The forms of the low-lying diagrams considered are shown in (a′) and (b′) of Fig. 8. Diagram (a′) is for the case α, $\beta=0f_{7/2}$, $0f_{5/2}$, $1p_{3/2}$, $1p_{1/2}$, with the condition that $\beta\neq 0f_{7/2}$ and contributes to Eq. (3.4). The case $\beta=k$ is shown in (b′) and is separated from (a′) because of its effective three-body character. Figures 8(a′) and 8(b′) give a total of 15 distinct diagrams to the violation of the ph transformation; the remaining low-lying diagrams are at least an order of magnitude smaller because they lie a minimum of $2\hbar\omega$ away from $0f_{7/2}$. The single-particle energy differences are recorded in Table V and are the same as those used by Kuo and Brown.[16]

The model for ^{48}Sc is one proton particle and one neutron hole in the $0f_{7/2}$ shell outside a ^{48}Ca core. The diagrams that violate in this case are of the type (a) in Fig. 8, which correspond to (a′) of the ^{42}Sc case, and (c) and (b), which have no pp transforms. Diagrams (c) and (b) contribute an additional nine terms for $\beta=0f_{7/2}$ and $\alpha=0f_{5/2}$, $1p_{3/2}$, $1p_{1/2}$ of an effective three-body nature to ^{48}Sc. The single-particle energy differences used in this case were obtained using the spectrum of ^{49}Sc for the proton differences and ^{49}Ca along with ^{47}Ca for the neutron energy differences. We use the values quoted by Kuo and Brown,[16] which include isospin effects in ^{49}Sc by Green.

The contributions of the second-order diagrams of Fig. 8 to the violation (2.15) are calculated using the following equations. For ^{48}Sc

$$\Delta E_J(a)=-\sum_{\alpha'\beta\mu}[\mu]W(jkkj;\mu J)\times\{\sum_{\lambda}W(jk\alpha'\beta;\mu\lambda)[jk\lambda]^{1/2}\alpha^{\lambda}(jk\alpha'\beta)\}^2/E_{\alpha'\beta}, \quad (4.1)$$

$$\Delta E_J(b)=\sum_{\alpha'}\{\sum_{\lambda}(-1)^{\lambda}[jk\lambda]^{1/2}W(k\alpha'kj;J\lambda)\times\alpha^{\lambda}(jk\alpha'k)\}^2/E_{j\alpha'}, \quad (4.2)$$

$$\Delta E_J(c)=\sqrt{2}[jk]\sum_{\alpha'\lambda\lambda'}(-1)^{\lambda-J}[\lambda\lambda']^{1/2}\{\delta_{\lambda\lambda'}[\lambda]^{-1}-(-1)^{k+\alpha'}W(kkk\alpha';\lambda\lambda')\}W(jkjk;J\lambda')\times\alpha^{\lambda}(jkj\alpha')\alpha^{\lambda'}(\alpha'kkk)/E_{j\alpha'}, \quad (4.3)$$

with $E_{j\alpha'}=E_j-E_{\alpha'}$. The α^{λ} are the off-diagonal multipole strengths (A3) of $\mathcal{V}_c$, which are calculated in the np formalism.

The contributions of the pp diagrams (a′) and (b′) are simply related to (4.1), as explained in (3.1)–(3.4).

We have taken, as approximations to $\mathcal{V}_c$ for this calculation, two sets of two-body effective matrix elements, which have been calculated by Kuo and Brown[16] and by Shakin *et al.*,[17] respectively. Both sets include the Brueckner ladder interaction $\mathcal{V}_B$; the Kuo-Brown set is the "renormalized" interaction which adds some core-excitation effects to $\mathcal{V}_B$. These core-excitation contributions, which are calculated to second order in $\mathcal{V}_B$, may be treated as *high-lying*, and therefore transform as $\mathcal{V}_c$.

The dilution effect, which is the near-cancellation of diagrams (a) and (a′) of Fig. 8, has negligible contribution for $\alpha'\neq i$. The remaining calculated terms are listed under "Perturbation" in Tables VI and VII. The results are given both in terms of the spectral violations ΔE_J [Eq. (2.15)] and in terms of the corresponding multipole violations

$$\Delta\alpha^{\lambda}\equiv\alpha^{\lambda}(^{48}\mathrm{Sc})-(-1)^{\lambda+1}\alpha^{\lambda}(^{42}\mathrm{Sc}), \quad (4.4)$$

where α^{λ} is defined in (1.3).

We have also carried the calculation of the violation to higher order in $\mathcal{V}_c$. An indication that this is necessary is given in the calculation by Kuo and Brown[16] of the spectrum of ^{42}Sc. They found large admixtures into some of the $(f_{7/2})^2$ states, which imply that second-order perturbation theory may be inadequate.

We have examined this question by including interactions $\mathcal{V}_c$ in the $2p$ excited states in Figs. 8(a′) and 8(b′) for the ^{42}Sc case. The complete series of such

[16] T. T. S. Kuo and G. E. Brown, Nucl. Phys. **A114**, 241 (1968).

[17] C. M. Shakin, Y. R. Waghmare, M. Tomaselli, and M. H. Hull, Jr., Phys. Rev. **161**, 1015 (1967); and (private communication).

TABLE V. The single-particle energy differences (E_j-E_α) for both neutron and protons is used in the calculations of diagrams in both ^{42}Se and ^{48}Sc (in MeV).

j	α	^{42}Sc		^{48}Sc	
$0f_{7/2}$		$(E_j-E_\alpha)_n$	$(E_j-E_\alpha)_p$	$(E_j-E_\alpha)_n$	$(E_j-E_\alpha)_p$
	$0f_{5/2}$	−6.5	−6.5	−8.38	−5.9
	$1p_{3/2}$	−2.1	−2.1	−4.48	−4.4
	$1p_{1/2}$	−3.9	−3.9	−6.58	−6.9

TABLE VI. Comparison of calculated contributions (in MeV) to the spectral violation [(1.7) and (4.5)]: (1) for ^{48}Sc, second-order perturbation, (2) for ^{42}Sc, second-order perturbation, (3) for ^{42}Sc, matrix calculation, all using RKB matrix elements. The total violations are given in terms of the differences ΔE_J: (1) − (2) and $\Delta\alpha^\lambda$: (1) − (3) in (4) and (5), respectively; (6) gives the experimental values, from Tables III and IV.

J	(1) Pert. $E_J(48)$	(2) Pert. $TE_J(42)$	(3) Matrix $TE_J(42)$	(4) Pert. ΔE_J	(5) Matrix ΔE_J	(6) Expt. ΔE_J
0	0.789	0.831	1.471	−0.042	−0.686	−0.868
1	−0.636	−0.368	−0.771	−0.269	0.132	−0.477
2	−0.045	−0.095	−0.040	0.049	−0.008	0.168
3	−0.186	0.019	0.069	−0.206	−0.258	−0.423
4	−0.057	0.261	0.366	−0.318	−0.424	−0.507
5	−0.055	0.230	0.356	−0.286	−0.411	−0.588
6	−0.115	0.236	0.461	−0.351	−0.575	−0.629
7	0.351	0.283	0.565	0.068	−0.212	−0.715
λ	$\alpha^\lambda(48)$	$(-1)^{\lambda+1}\alpha^\lambda(42)$	$(-1)^{\lambda+1}\alpha^\lambda(42)$	$\Delta\alpha^\lambda$	$\Delta\alpha^\lambda$	$\Delta\alpha^\lambda$
0	0.0	+0.181	+0.330	−0.181	−0.330	−0.537
1	0.157	0.104	0.210	0.053	−0.053	−0.155
2	0.088	−0.050	−0.058	0.138	0.146	0.030
3	0.064	0.010	0.011	0.054	0.053	0.023
4	0.060	+0.056	+0.056	0.004	0.004	−0.084
5	−0.027	−0.076	−0.110	0.049	0.083	0.100
6	0.055	+0.050	+0.102	0.005	−0.047	−0.073
7	−0.146	−0.095	−0.197	−0.051	0.051	−0.062

TABLE VII. Comparison of the experimental spectral violations [(1.7) and (4.5)] with the calculated values, using the RKB and SWTH matrix elements. For each case, the second-order perturbation (1) and matrix calculation (2) results are listed (in MeV).

		RKB		SWTH	
$J\backslash\Delta E_J$	Expt.	(1)	(2)	(1)	(2)
0	−0.868	−0.042	−0.686	−0.097	−0.416
1	−0.477	−0.268	0.132	−0.310	0.069
2	0.168	0.049	−0.008	−0.067	−0.372
3	−0.423	−0.206	−0.258	−0.184	−0.145
4	−0.507	−0.318	−0.424	−0.358	−0.269
5	−0.588	−0.286	−0.411	−0.229	−0.134
6	−0.629	−0.351	−0.575	−0.324	−0.385
7	−0.715	0.068	−0.212	−0.013	−0.277
$\lambda\backslash\Delta\alpha^\lambda$					
0	−0.537	−0.181	−0.330	−0.200	−0.252
1	−0.155	0.053	−0.053	0.048	−0.043
2	0.030	0.138	0.146	0.092	0.005
3	0.023	0.054	0.053	0.038	0.026
4	−0.084	0.004	0.004	0.007	0.055
5	0.100	0.049	0.083	0.053	0.028
6	−0.073	0.005	−0.047	0.030	0.020
7	−0.062	−0.051	0.051	−0.033	0.084

TABLE VIII. Comparison of several average quantities (in keV) calculated using the experimental ^{48}Sc spectrum and the ^{42}Sc spectrum with corrections. (1), experimental ^{48}Sc; (2), shell-model transform (1.2) of ^{42}Sc; (3) and (4), transform (1.2) plus many-body corrections, using matrix calculation.

	^{48}Sc Expt.	$T(^{42}$Sc) Expt.	$T(^{42}$Sc) +RKB	$T(^{42}$Sc) +SWTH
rms deviation	···	580	310	415
$(2J+1)$-weighted rms deviation	···	584	296	386
Monopole	895	1423	1093	1171
Isospin splitting $(T=3, 4)$	6077	6413	6438	6243
$\bar{V}_1$	−40	−530	−188	−293
$\bar{V}_0$	−1560	−2133	−1798	−1854

ladder diagrams is equivalent to the solution of a secular matrix problem, in the orbital space jk, $j\alpha$, αk, and $\alpha\beta$. This is similar to the matrix problem treated in Ref. 16, except that we omit $(g_{9/2})^2$, which we consider "high-lying." We may compare the result of this calculation with the perturbation calculation discussed above, as follows: We diagonalize the matrix and identify the eigenvalues associated with $(f_{7/2})^2$. Since this matrix includes the $\alpha\beta$ states $(\alpha\neq j)$ which we have eliminated from our perturbation results, we subtract from these eigenvalues the eigenvalues of a reduced shell-model matrix in the space jk, $\alpha\beta$ $(\alpha\neq j, \beta\neq k)$. This difference of eigenvalues

$$E_J(42)\equiv E_J(\text{matrix})-E_J(\text{matrix, no } j\alpha,\ \alpha k) \quad (4.5)$$

is the energy shift due to the sum of violating diagrams in ^{42}Sc. The contribution to the violation (2.15) is given by the transform $TE_J(42)$ [Eq. (1.2)]. These matrix results are shown in Table VI for the renormalized Kuo-Brown (RKB) two-body matrix elements. By comparison with the second-order perturbation results listed in the table, we see that the higher-order terms of the series make considerable difference to the results.

A complete matrix calculation for ^{48}Sc using the same (f-p shell) orbits is neither feasible nor desirable. We have investigated the summation of series of ph diagrams, of the types (a) and (b) of Fig. 8, including ladders of interactions in the intermediate states, similar to those which are significant in ^{42}Sc. We find that, unlike the ^{42}Sc case, these higher-order terms do not make a major contribution to the energies $E_J(48)$. Apparently the configuration mixing in ^{48}Sc is weak enough to be described adequately in second order. This can be understood in part by the fact (Table V) that the single-particle excitation energies are higher in ^{48}Sc than in ^{42}Sc. This holds particularly for the $p_{3/2}$ level, which causes much of the strong admixing in ^{42}Sc. For these reasons, we have used the second-order perturbation results for ^{48}Sc in Tables VI and VII. We are investigating further the higher-order structure of ^{48}Sc.

The resulting violations $(\Delta E_J, \Delta\alpha^\lambda)$ computed using both the second-order and the matrix results for ^{42}Sc are listed in Tables VI and VII, and may be compared with the experimental values, taken from Tables II and IV. It is clear that the matrix results may account for a large part of the experimental violation. For example, the rms deviations between the experimental and calculated spectra of ^{48}Sc are given in Table VIII. The 580-keV rms deviation obtained by simply transforming (1.2), the ^{42}Sc spectrum, is reduced by $\frac{1}{2}$ for the RKB calculation and by $\frac{1}{3}$ for Shakin *et al.* (SWTH).[17]

We note that in the calculations, as in the experimental case, the monopole is the largest violating term, and contributes most to the $[J]$-weighted rms deviation (537 out of 584 keV, experimental).

A way of measuring the quality of all the calculated multipoles is given as follows: We consider the $\Delta\alpha^\lambda$ as the components of an eight-dimensional vector **A**. Then our measure is given by two numbers: the ratio of norms of the theoretical vector $\mathbf{A}(t)$ and experimental vector $\mathbf{A}(e)$:

$$N=|\,\mathbf{A}(t)\,|/|\,\mathbf{A}(e)\,|, \qquad |\,\mathbf{A}^2\,|=\sum_\lambda(\Delta\alpha^\lambda)^2, \quad (4.6a)$$

and the scalar product of the normed vectors:

$$X=\mathbf{A}(t)\cdot\mathbf{A}(e)/|\,\mathbf{A}(t)\,|\,|\,\mathbf{A}(e)\,|,$$
$$\mathbf{A}(t)\cdot\mathbf{A}(e)=\sum_\lambda\Delta\alpha^\lambda(t)\Delta\alpha^\lambda(e). \quad (4.6b)$$

N is a measure of the magnitude of the calculated violations, while X is a measure of the direction in the eight-dimensional space, both relative to the experimental numbers. A perfect fit to experiment is $N=X=1$. We weight equally each multipole in (4.6), since the strengths are normalized to give equal contribution to the $[J]$-weighted rms deviation:

$$|\,\mathbf{A}(e)-\mathbf{A}(t)\,|$$
$$=\{\sum_J[J][\Delta E_J(e)-\Delta E_J(t)]^2/\sum_J[J]\}^{1/2}. \quad (4.7)$$

It is also useful to separate out the monopole term and take the remaining multipole strengths as the components of a seven-dimensional vector, and calculate

TABLE IX. Values of the quality measures N, X [see Eq. (4.6)] calculated for RKB and SWTH matrix elements, given both including (eight-dimensional) and omitting (seven-dimensional) the monopole term. A perfect fit to experiment would be $N=X=1$.

Measure	RKB	SWTH
With monopole (eight-dimensional)		
N	0.659	0.477
X	0.889	0.828
Without monopole (seven-dimensional)		
N	0.863	0.520
X	0.488	−0.042

new values of N and X. Both sets of measures are given in Table IX, for the matrix calculations with RKB and SWTH matrix elements. One sees that when one includes the monopole, the SWTH calculations are a slightly poorer fit to experiment than the RKB, but when the monopole is excluded, the SWTH are much poorer. This is reflected in the signs of the $\Delta\alpha^\lambda$ in Table VII.

Another measure of the quality of the calculation may be obtained by comparing the average isospin structure of ^{42}Sc and ^{48}Sc. We define the $[J]$ average interaction for fixed isospin T, for the pp system:

$$\bar{V}_T=\sum_J[J]\{1-(-1)^{T+J}\}E_J(\mathrm{pp})/\sum_J[J]\{1-(-1)^{T+J}\}. \tag{4.8}$$

The difference $\bar{V}(1)-\bar{V}(0)$ gives the average isospin splitting in ^{42}Sc. For ^{48}Sc we may obtain the $[J]$ average isospin splitting between the $T=4$ $(J=0)$ and $T=3$ $(J=1$–$7)$ levels, using

$$\bar{E}(4)-\bar{E}(3)=4[\bar{V}(1)-\bar{V}(0)]. \tag{4.9}$$

[This equation is a special case of Eq. (6-21) of Ref. 18.] In Table VIII we compare the isospin splitting for ^{48}Sc [left-hand side of (4.9)] with that obtained from the ^{42}Sc spectrum [right-hand side of (4.9)], and find a violation of (4.9) by 336 keV. By including the violating interaction, the effective value of $4[\bar{V}(1)-\bar{V}(0)]$ is shifted by -170 keV for the SWTH calculation, improving the agreement. However, here the RKB result is in the wrong direction. In Table VIII we also list the "effective" $\bar{V}(T)$ for ^{48}Sc, defined by Eq. (4.9) (and the monopole shift).

5. CONCLUSIONS

The theory presented seems to provide a basis for quantitative understanding of the discrepancy between the experimental spectrum of ^{48}Sc and that predicted by applying relation (1.2) to the spectrum of ^{42}Sc. The agreement which is achieved indicates that the theoretically predicted violations are physical effects and do account for the major portion of the discrepancy. It should be stressed again that the monopole is the largest part of the discrepancy. Bertsch[15] has calculated the contribution of three-body terms, similar to those of Fig. 7(c), to the binding energies of the closed-shell nuclei ^{48}Ca and ^{56}Ni. The additional energy may be simply related to the ^{42}Sc contribution to the monopole discrepancy in our problem, and the numerical results are in approximate agreement.

We note that the calculated results are sensitive to the choice of $\mathcal{V}_c$ matrix elements, and that the RKB matrix elements lead to generally better agreement with experiments than do the SWTH matrix elements.

In principle, to improve the calculations, one should include more intermediate configurations and higher orders in the interaction $\mathcal{V}_c$. This we have done in part with the matrix calculation for ^{42}Sc. We are investigating similar extensions in ^{48}Sc. However, we foresee the problem, which also occurs elsewhere in spectroscopy, that this procedure is not convergent if there are low-lying configurations involving excitation of many particles ("collective" states). The Kuo-Brown renormalization was intended to include effects of the latter. Perhaps this is why we find better agreement in the signs of the multipoles for RKB than for SWTH, which has no core polarization. We have seen that the violation of the relation (1.2) may be thought of as due to configuration mixing. However, we have also seen that only *particular* configurations, which either occur only at one end of the shell or whose admixed strength changes with the core, contribute to the violation. For example, the early calculation by Pandya and French[6] of ^{38}Cl-^{40}K included some of the first kind of terms. Other configuration mixtures, which we have characterized as *high-lying*, have little effect on the ph relation. Conversely, the degree of agreement of experimental spectra with relation (1.2) is not a measure of configuration purity.

Clearly a similar approach can be applied to other spectral relations in the shell model, for example, the transformation of a pp to a hh spectrum. Further work in this direction is under way, and will be reported in a subsequent paper.

ACKNOWLEDGMENTS

The authors would like to thank Professor J. B. French for careful reading and criticism of the manuscript, and Dr. J. P. Svenne and Dr. J. C. Parikh for supplying the matrix elements of Shakin *et al.*[17] in the jj shell-model form.

APPENDIX A

We discuss in this appendix the multipole form of the two-body interaction and also the form of the ph transformation in the multipole representation.[5] An example of a calculation of a perturbation diagram is also worked out, using the multipole formalism.

Consider any two-body interaction which conserves the total angular momentum J of a system of particles; this can be written in the second-quantized form

$$V_2=\sum_{lmnr,J}[J]^{1/2}\langle lm;J\mid V_2\mid nr;J\rangle \times\left[\frac{(A_l\times A_m)^J}{(1+\delta_{lm})^{1/2}}\times\frac{(B_n\times B_r)^J}{(1+\delta_{nr})^{1/2}}\right]^0. \tag{A1}$$

The operators A_n and B_n are the spherical-tensor creation and destruction operators, respectively, for a particle in the state n, where n may stand for the orbital quantum numbers (n,l,j,t_3). The tensor operator $(A_l\times A_m)^I$ creates two particles in the single-particle states l and m, coupled to total angular momentum I.

[18] J. B. French, in *Nuclear Structure*, edited by Hossain *et al.* (North-Holland Publishing Co., Amsterdam, 1967), p. 85.

The normalization is chosen so that the double-barred matrix element (dbme) of the operator portion of (A1) in the state $(jk)^J$ is unity for l, $n=j$ and m, $r=k$, with $j\neq k$. The coefficients $\langle jk;J\,|\,V_2\,|\,jk;J\rangle$ are the conventional two-body matrix elements of V_2.

An alternative form of V_2, which facilitates the comparison of the experimental violation of the ph transformation with those calculated using the results of Sec. 2, is obtained by means of an angular momentum recoupling of the operator portion of V_2. This recoupled version of the two-body interaction is written in (A2) in its *multipole form*

$$V_2=\sum_{lmnr,\lambda}[lm\lambda]^{1/2}\alpha^\lambda(lmnr)\,\frac{u^\lambda(ln)\cdot u^\lambda(mr)}{(1+\delta_{lm})^{1/2}(1+\delta_{nr})^{1/2}}\,. \tag{A2}$$

The expansion coefficients $\alpha^\lambda(lmnr)$ are the multipole strengths of tensoral rank λ, and the $u^\lambda(ln)$ are the diagonal Racah unit tensors that operate in the single-particle space such that their dbme is unity:

$$\langle l\,||\,u(l'm')\,||\,m\rangle=\delta_{ll'}\delta_{mm'},$$

with the single-particle normalization

$$\langle l\,||\,1\,||\,m\rangle=\delta_{lm}[l]^{1/2}=\delta_{lm}(2l+1)^{1/2}.$$

The expansion coefficients of (A2) are related to those of (A1) by means of a Racah coefficient which determines the angular momentum recoupling involved in going from the one form to the other:

$$\alpha^\lambda(lmnr)=[\lambda/lm]^{1/2}\sum_J(-1)^{l+r-J}[J]W(lmnr;J\lambda)\times\langle lm;J\,|\,V_2\,|\,nr;J\rangle. \tag{A3}$$

This equation relates the multipole strengths to the standard two-body matrix elements of the interaction and can be inverted to yield

$$\langle lm;J\,|\,V_2\,|\,nr;J\rangle=[lm]^{1/2}\sum_\lambda[\lambda]^{1/2}(-1)^{l+r-J}\times W(lmnr;J\lambda)\alpha^\lambda(lmnr). \tag{A4}$$

The transformations (A3) and (A4) may be easily derived using (A1) and the operator form of the Racah unit tensor in (A2):

$$u^\lambda(ln)=[\lambda]^{-1/2}(A_l\times B_n)^\lambda. \tag{A5}$$

The ph transformation can be written in terms of multipoles if we transform the particle A_m and B_l to hole operators, using[5] $B_l=(-1)^{2l}A_l(\mathrm{h})$ and $A_m=B_m(\mathrm{h})$. Now the pp unit tensor in (A2) may be rewritten, by commuting A_m, B_r, in the form

$$u^\lambda(mr)=(-1)^{m-r-\lambda+1}u^\lambda(r^{-1}m^{-1})+[m]^{1/2}\delta_{mr}\delta_{0\lambda}. \tag{A6}$$

With this replacement of the unit tensor in (A2) the two-body interaction take the ph form

$$V_2=\sum_{lmnr,\lambda}(-1)^{m-r-\lambda+1}[lm\lambda]^{1/2}\alpha^\lambda(lmnr)\times u^\lambda(ln)\cdot u^\lambda(r^{-1}m^{-1})+\sum_{mnl}[m][l]^{1/2}\alpha^0(lmnm)u^0(ln). \tag{A7}$$

The extra one-particle term arises from the commutation of A_m with B_r and is seen to be a monopole term. It should be included in the definition of the single-particle energy U, so that it does not contribute to the two-body interaction of the particle and hole. For this reason the one-body part was dropped in our definition of the ph interaction energy in Sec. 1.

Comparing the first term of (4.7) with (A2) immediately leads to a pp-ph transformation for multipole coefficients:

$$\alpha^\lambda(lmnr)=(-1)^{m-r-\lambda+1}\alpha^\lambda(lm^{-1}nr^{-1}). \tag{A8}$$

The recoupling (A4) leads to the more familiar form of the pp-ph transformation

$$\langle r^{-1}l;I\,|\,V_2\,|\,m^{-1}n;I\rangle=-\sum_J[J]W(lmrn;IJ)\times\langle lm;J\,|\,V_2\,|\,nr;J\rangle. \tag{A9}$$

Note that odd-λ and even-λ multipole strengths transform differently in (A8); with $m=r$, for even λ they change sign, for odd they do not.

Diagrams may be calculated using the multipoles defined by (A2) with the least amount of recoupling. As an example, consider diagram (b) of Fig. 6; the interaction V_2 in this case is replaced by the reaction matrix $\mathcal{U}_B$ (see Sec. 2), which can also be written in forms (A1) and (A2). The latter form for the contributing portions of the two interactions are, from the top down,

$$\mathcal{U}_{\mathrm{top}}=\sum_\lambda[jk\lambda]^{1/2}\alpha^\lambda(jk\alpha\beta)u^\lambda(j\alpha)\cdot u^\lambda(k\beta),$$

$$\mathcal{U}_{\mathrm{bottom}}=\sum_{\lambda'}[jk\lambda']^{1/2}\alpha^{\lambda'}(\alpha\beta jk)u^{\lambda'}(\alpha j)\cdot u^{\lambda'}(\beta k),$$

so that the matrix element corresponding to this diagram may be written

$$\begin{aligned}\langle jk^{-1};J\,|\,\mathcal{U}_{\mathrm{top}}(Q_{\alpha\beta}/E_{\alpha\beta})\mathcal{U}_{\mathrm{bottom}}\,|\,jk^{-1};J\rangle&=([jk]/E_{\alpha\beta})\sum_{\lambda\lambda',\mu\nu}[\lambda\lambda']^{1/2}\alpha^\lambda(jk\alpha\beta)\alpha^{\lambda'}(\alpha\beta jk)\\&\times\langle jk^{-1};J\,|\,u^\lambda(j\alpha)\cdot u^\lambda(k\beta)\,|\,\alpha[\beta(k^{-2})^\nu]^\mu;J\rangle\\&\times\langle\alpha[\beta(k^{-2})^\nu]^\mu;J\,|\,u^{\lambda'}(\alpha j)\cdot u^{\lambda'}(\beta k)\,|\,jk^{-1};J\rangle.\end{aligned}$$

This expression can be evaluated by decoupling the spaces, using

$$\begin{aligned}\langle jk^{-1};J\,|\,u^\lambda(j\alpha)\cdot u^\lambda(k\beta)\,|\,\alpha[\beta(k^{-2})^\nu]^\mu;J\rangle&=(-1)^{j+\mu-J}W(jk\alpha\mu;J\lambda)\langle j\,||\,u^\lambda(j\alpha)\,||\,\alpha\rangle\\&\times\langle k^{-1}\,||\,u^\lambda(k\beta)\,||\,\beta(k^{-2})^\nu;\mu\rangle,\end{aligned}$$

so that the final result is

$$\langle jk^{-1};J\,|\,\mathcal{V}_{\rm top}(Q_{\alpha\beta}/E_{\alpha\beta})\mathcal{V}_{\rm bottom}\,|\,jk^{-1};J\rangle$$
$$=-\sum_{\mu}[\mu]W(jkkj;\mu J)\{\sum_{\lambda}[jk\lambda]^{1/2}$$
$$\times W(jk\alpha\beta;\mu\lambda)\alpha^{\lambda}(jk\alpha\beta)\}^{2}E_{\alpha\beta}^{-1}. \quad \text{(A10)}$$

This expression shows that the diagram and its matrix elements do transform properly, unless, of course, the intermediate state is *low-lying*. All the diagrams of Sec. 3 are calculated using this procedure.

APPENDIX B

In this appendix we shall prove that terms in $\mathcal{V}$, designated as *high-lying* (Sec. 2), do transform by (1.5). We shall use the diagrammatic form of perturbation theory, in which one associates diagrams with individual terms in the perturbation expansion of the diagonal matrix element of $\mathcal{V}$ [Eq. (2.1)] (see Refs. 7 and 8).

Consider diagrams for the pp matrix elements (2.2) of the form shown in Fig. 4(a), where the blocks schematically represent the possible interactions in that given time interval. This kind of diagram is associated with what we have called a high-lying term in Sec. 2, if the blocks contain *no valence* lines, and if the denominators are sufficiently large, as discussed. We have also restricted the diagram to be linked in that there will be a connection of the valence lines through at least one interaction. This allows us to use the linked-valence formalism[7] (2.1′), which can only be done in a diagrammatic formalism. The projection method in (2.3)–(2.12) does not separate linked and unlinked terms.

The diagram is constructed as follows: At the vertex t_0 the interaction V_2 takes the particle line k into the block (1), which begins with two particle lines α, β, and a hole line μ^{-1}. We can write this operation as [see Appendix A, Eq. (A1)]

$$\sum_{L_1}\langle\alpha\beta;L_1\,|\,V_2\,|\,\mu k;L_1\rangle\langle S_0;J_0\,|$$
$$\times[(A_\alpha\times A_\beta)^{L_1}\times(B_\mu\times B_k)^{L_1}]^0\,|\,k\rangle, \quad \text{(B1)}$$

where S_0 stands for the coupling of α, β, and μ^{-1} with total angular momentum J_0. Similarly, at vertex t_1 we will encounter a matrix element of the same form as (B1), but with B_j replacing B_k. At vertices t_2 and t_3, the particle creation and destruction operators in (B1) are reversed, and we obtain A_j and A_k, respectively. The matrix element corresponding to the entire diagram (a) of Fig. 4 will contain four factors of the form (B1), multiplied by a number of factors corresponding to interactions in the blocks, and the energy denominators which give the propagation of the system between interactions.

Because, by assumption, we are dealing with *high-lying* terms, the operators A_k and B_k (and also A_j and B_j) occur only once in the expression for the diagram, and only at the "corner" vertices as discussed above. It is convenient, in a discussion of the transformation of particle k into a hole, to bring the operators A_k and B_k together in the expression for the matrix element for the entire diagram (a) of Fig. 4. This involves implicitly commuting A_k and B_k over any other operators which appear (but not over each other), and recoupling the angular momenta from the forms (B1) so that A_k and B_k form a unit tensor [see (A4)]:

$$u^{\lambda}(kk)=[\lambda]^{-1/2}(A_k\times B_k)^{\lambda}.$$

Then the matrix element can be written in the form

$$E_D(jk;J)=\langle jk;J\,|\,\mathcal{V}_c(D)\,|\,jk;J\rangle \quad \text{(B2a)}$$
$$=\sum_{\lambda}[T^{\lambda}\times u^{\lambda}(kk)]^0, \quad \text{(B2b)}$$

where T^{λ} is a spherical-tensor operator of rank λ, which will contain A_j, B_j, and the other operators, matrix elements, and denominators implied by the structure of the diagram.

Now consider the matrix elements of the operator $\mathcal{V}_c(D)$ in (B2b) in the ph state $(j,k^{-1};I)$:

$$\langle jk^{-1};I\,|\,\mathcal{V}_c(D)\,|\,jk^{-1};I\rangle. \quad \text{(B3)}$$

This can be calculated, following the discussion in Appendix A, by transforming $u^{\lambda}(kk)$ to $u^{\lambda}(k^{-1}k^{-1})$ using (A5). The operator (B2b) takes the form [see (A6)]

$$\mathcal{V}_c(D)=\sum_{\lambda}[T^{\lambda}\times u^{\lambda}(k^{-1}k^{-1})]^0(-1)^{\lambda+1}+[k]^{1/2}T^0. \quad \text{(B4)}$$

If we take the matrix element (B3) using the separation (B4), we obtain two terms which can be identified with Figs. 4(b) and 4(c), respectively. That is, in the first term of (B4), the order of A_k and B_k have been reversed, corresponding to the interchange of particle and hole roles at the vertices t_0 and t_2. The second term comes from the commutation of A_k and B_k, and corresponds to the "Pauli correction" (disconnected) of Fig. 4(c). Since this diagram contributes to the single-particle energy relative to the new (filled k shell) core, we do not include it in the ph interaction energy, which is therefore contributed by the first term in Fig. 4(b).

The identification of the matrix elements (B3) of the two terms of (B4) with the ph diagrams in Figs. 4(b) and 4(c) is possible only because the same operator T^{λ} appears in both pp and ph diagrams. That follows from the fact that only external lines have been altered in going from Fig. 4(a) to Figs. 4(b) and 4(c). This does formally change the energy denominators, that is, if, for some intermediate "time," the denominator in Fig. 4(a) is

$$E_0-H_0=E_j+E_k-E_{\rm int}, \quad \text{(B5a)}$$

then the denominator in Fig. 4(b) [of 4(c)] at the same "time" is

$$(E_0-H_0)'=E_j+E_k^{-1}-(E_{\rm int}+2E_k^{-1})$$
$$=E_j-E_k^{-1}-E_{\rm int}', \quad \text{(B5b)}$$

where $E_{\rm int}$ is the excitation energy of the intermediate state in the pp diagram and $E_{\rm int}'$ is the excitation energy of the same particles in the ph diagram. We would have (B5a) = (B5b) if $E_{k^{-1}} = -E_k$ and $E_{\rm int}' = E_{\rm int}$. Although these conditions do not hold in general, we will have

$$E_0 - H_0 = (E_0 - H_0)' \tag{B6}$$

under the condition that we have described as *high-lying*, that is, if each of the energy denominators is larger than the variation in E_k or $E_{\rm int}$.

Finally, we find that the ph interaction energy contributed by Fig. 4(b) may be written

$$E_D(jk^{-1};I) = \sum_\lambda (-1)^{\lambda+1} \langle jk^{-1};I \mid \times[T^\lambda \times u^\lambda(k^{-1}k^{-1})]^0 \mid jk^{-1};I\rangle, \tag{B7}$$

which can also be written as a transform of the contribution (B2a) of diagram (a) of Fig. 4 to the pp interaction energy, following (A8):

$$E_D(jk^{-1};I) = -\sum_J [J] W(jkkj;IJ) E_D(jk;J). \tag{B8}$$

This completes the proof of the theorem that *high-lying* diagrams contribute to the *conserving* valence effective interaction $\mathcal{V}_c$ [Eqs. (1.5) and (1.6)].

If the diagram (a) of Fig. 4 has vertices t_0 and t_2 interchanged, then there will be two particle lines between t_2 and t_0. Then the "Pauli-correction" (disconnected) diagram appears for the pp case, and the roles of pp and ph are interchanged in the above proof.

Finally, we note that the restriction that the particle operators A_j and B_j must appear *only* once each is not necessary for the proof, since these operators are contained in T^λ, and do not change in the ph transformation. This implies that our definition of high-lying terms is somewhat more restrictive than necessary. This has no practical effect on the calculation of the *violating* contributions, however, since conserving terms would cancel in (2.15).

PHYSICAL REVIEW VOLUME 187, NUMBER 4 20 NOVEMBER 1969

Three-Body Model of Li^6 and Deuteron–Alpha-Particle Scattering*

PAUL E. SHANLEY
Department of Physics, University of Notre Dame, Notre Dame, Indiana 46556
(Received 27 June 1969)

The properties of Li^6 and deuteron–α-particle scattering are studied in an exact three-particle model in which the neutron, proton, and α particle interact through separable two-body forces. The α particle is assumed to be structureless, and Coulomb effects are neglected. As a representation of the nucleon–α-particle interaction, a three-term separable potential fit to low-energy neutron–α-particle scattering is introduced in the partial waves $s_{1/2}$, $p_{3/2}$, and $p_{1/2}$. The $s_{1/2}$ interaction is taken to be repulsive, while the other two are attractive. The three-body formalism of Amado is generalized to allow spin-dependent two-body interactions in an arbitrary partial wave. Numerical solution of the resulting three-body equations gives the binding energies of the $T=0$ and $T=1$ states of Li^6 as well as phase shifts, angular distributions, and deuteron polarization in d-α scattering, and also the total cross section for $d+\alpha \to n+p+\alpha$ up to 30 MeV. Most of the calculations have used only an s-wave n-p interaction, but a limited number have been done with the d state of the deuteron included in order to assess its importance. Given the assumptions of the model, the agreement of the calculated quantities with experiment is very good. Some discussion of the results with respect to phenomenological optical-model fits to deuteron-nucleus scattering is also given.

I. INTRODUCTION

In recent years, considerable progress has been made in understanding the three-nucleon system by the use of the separable approximation in equations of the Faddeev type.[1] In this approximation a small number of separable two-body amplitudes are adjusted to fit low-energy nucleon-nucleon scattering and these amplitudes are subsequently used as input in some form of three-body equation. Numerical solution of these equations has yielded results in rather good agreement with experiment but the complexity of the nucleon-nucleon interaction and complications of spin have prevented a really complete calculation from being carried out. What has been learned from this work is that one may successfully employ quite simple two-body interactions if three-body effects are treated exactly. In this paper we carry out a similar analysis[2] for a system consisting of a neutron, proton, and α particle. The spinless nature of the α particle reduces somewhat the complications which hamper a complete treatment of the problem of three nucleons.

* Research supported in part by the National Science Foundation under the University Science Development Program and by the U.S. Atomic Energy Commission.

[1] For a review, see *Three Particle Scattering in Quantum Mechanics*, edited by J. Gillespie and J. Nuttall (W. A. Benjamin, Inc., New York, 1968).

[2] A short account of this work appeared in P. E. Shanley, Phys. Rev. Letters 21, 627 (1968).